AT-01-10-4

A Simplified Analysis of Radiant Heat Loss Through Projecting Fenestration Products

John L. Wright, Ph.D., P.Eng.
Member ASHRAE

ABSTRACT

Current window analysis algorithms can deal with many features, including low-e coatings and substitute fill gases. These methods were developed for products with planar glazings. Results can be generated for projecting products such as greenhouse windows, but the indoor-side heat transfer coefficient must be reduced to reflect differences in convection and radiant exchange for this geometry. Two simplified models are developed for radiant heat loss to projecting windows and are shown to agree well with a pseudo three-dimensional multi-element computer-based calculation. It is confirmed that the indoor-side heat transfer coefficient does not need to be accurately known to characterize a well-insulated window. More research is needed to quantify indoor-side convective heat loss before radiant exchange models can be verified and projecting products can be well characterized in general.

INTRODUCTION

A variety of calculation techniques have been developed for the thermal analysis of building envelope components. In particular, it is now common to compute the indices of merit for fenestration products using one or more of several pieces of software that are widely available. This approach, used in lieu of thermal testing, saves a significant amount of time and money regardless of whether the work is undertaken for product design, code compliance, or to generate information for marketing purposes.

Two computer programs are widely used for one-dimensional center-glass glazing system analysis. These are VISION (e.g., Wright and Sullivan 1995) and WINDOW (e.g., Finlayson et al. 1993). VISION is specified by the Canadian Standards Association (CSA 1993) and WINDOW is used for certification in the United States (NFRC 1991). Other programs are used for the two-dimensional analysis of frame and edge-glass heat transfer.

Current center-glass analysis algorithms can deal with many useful features, including coatings and substitute fill gases. These algorithms were developed for modeling windows built with planar (i.e., flat) glazings and are well suited for the analysis of the vast majority of product configurations, such as picture, casement, and sliding windows. Only the domed skylight must be excluded.

Results can be readily obtained for projecting products, such as greenhouse or garden windows, as long as the window consists of planar segments. For example, the U-factor U_i for each of n segments can be determined and combined to yield the U-factor, U, for the entire product. This is done by using the following energy balance as a definition for U.

$$q = \left(\sum_{i=1}^{n} U_i \cdot A_i \right) \Delta T = U \cdot A_p \cdot \Delta T \qquad (1)$$

where q is the heat loss through the window driven by ΔT, the indoor-outdoor temperature difference, A_i is the area of the ith window segment (projected to the plane of the segment in question), and A_p is the area of the window (projected to the plane of the wall). A_p is usually taken as the rough wall opening minus installation clearances. Rearranging Equation 1, we get the following:

$$U = \frac{\sum_{i=1}^{n} U_i \cdot A_i}{A_p}. \qquad (2)$$

John L. Wright is an associate professor, associate chair Undergraduate Studies, and manager of the Advanced Glazing System Laboratory, Department of Mechanical Engineering, University of Waterloo, Ontario, Canada.

Note that although U_i is based on A_i, as might be expected, U is based on the projected area of the window A_p and not on the surface area A_s. This is done in order to provide a meaningful comparison between different products that may occupy the same opening in the building envelope. A higher value of U is obtained because U is based on A_p and not A_s. This effect is larger for more strongly projecting products, i.e., products with a large ratio of surface to projected area, A_s/A_p. This is illustrated by rewriting Equation 2 in terms of A_s/A_p and assuming that A_s can be estimated by summing the individual values of A_i.

$$U = \frac{\sum_{i=1}^{n} U_i \cdot A_i}{\sum_{i=1}^{n} A_i} \cdot \frac{A_s}{A_p} \tag{3}$$

The first fraction on the right-hand side of Equation 3 is just the U-factor of the window based on surface area (i.e., the surface-area weighted average of the component-area U-factors), and the second fraction converts this value to a U-factor based on A_p. The area ratio A_s/A_p will always be greater than unity and can be seen as a penalty for the extra area that a projecting product presents to the environment. This idea can be demonstrated more clearly by considering a projecting product where U_i is the same for each window segment. In this case U_i can be removed from the summation and Equation 3 simplifies to

$$U = U_i \cdot \frac{A_s}{A_p}. \tag{4}$$

Equations 3 and 4 show that the U-factor of a projecting product will consistently be greater than the U-factor of its individual segments because of the penalty associated with increased surface area. The difference will be substantial for products with large surface-to-projected area ratios. However, it has also been recognized that some of this penalty is offset because of the corresponding differences in indoor-side heat transfer coefficient, h_{in}. Consider the heat flux to the indoor-side window surface, q_i''. It can be expressed in terms of h_{in}.

$$q_i'' = h_{in}(T_r - T_g) \tag{5}$$

where T_g represents the window surface temperature and T_r represents both the air temperature and surface temperature of the room, which are assumed to be equal. The heat transfer coefficient h_{in} can be expressed in terms of its convective and radiant components, h_c and h_r.

$$h_{in} = h_c + h_r. \tag{6}$$

A projecting product will have a lower value of h_{in} than the similar nonprojecting product for two reasons. First, h_r will decrease as A_s/A_p is increased from unity. A flat window "sees" only the indoor environment. In contrast, the indoor surfaces of a projecting window exchange radiation not only with the indoor environment but also with other parts of the window itself. There can be no net heat transfer from one part of the window to the other if the various window segments are all at the same temperature. Thus, as A_s/A_p increases and the window sees more of itself and less of the indoor environment, h_r is reduced. Second, as A_s/A_p is increased, h_c will decrease because the movement of air near the window surfaces will be restricted. The reduced airflow may manifest itself as stagnant regions in the more remote corners of the window recess or as recirculation zones or may exhibit other interesting and unusual flow patterns but will, in general, reduce h_c whether the flow is forced convection or natural convection.

Very little information is available to determine h_c for projecting products. Results pertaining to convection over a flat plate exist and are applied routinely to the analysis of more conventional windows. The detail of local variation in h_c was examined by Curcija and Goss (1993), but the results are also restricted to the analysis of conventional windows ($A_s/A_p \approx 1$) although the effect of small amounts of glazing setback was included.

One calculation standard (CEN/ISO 1999) also recognizes the effect of variation in heat transfer near the recessed corners of conventional windows and prescribes reduced values of h_{in} in these locations to obtain more accurate estimates of frame U-factor.

PREVIOUS RESULTS

Various computer programs offer a two-dimensional numerical conduction analysis that can be used to model frame and edge-glass heat transfer. One of these programs (Arasteh 1997) offers the option of a more complicated and very intricate model of radiant exchange between a multiplicity of indoor-side window surfaces (every surface corresponding to the exposed elements used in the finite element solution of conductive frame heat transfer) and the indoor environment. This calculation, based on a two-dimensional algorithm, is applied to a variety of vertical and horizontal cross sections of projecting windows to provide a pseudo three-dimensional analysis. In one study, U-factors for greenhouse windows were calculated with and without this multi-element model (Arasteh et al. 1998). The calculated results were also compared to measured results. In the case of a poorly insulated greenhouse window (3 mm clear – 6.7 mm air – 3 mm clear, solid aluminum frame, $A_s/A_p = 2.11$), the multi-element model predicted a U-value 21% lower than the U-value calculated when the self-viewing nature of the window was not considered (i.e., $U = 7.95$ W/m^{2}K versus $U = 10.11$ W/m^{2}K, respectively). Measured results from two different laboratories for the same window were $U = 7.65$ and 6.09 W/m^{2}K. When a more highly insulated greenhouse window was examined (low-e, 13 mm argon, PVC frame, $A_s/A_p = 1.83$), application of the more complicated multi-element model reduced the calculated value of U by 13%, from 4.32 to 3.75 W/m^{2}K. Only one measurement was available for the second window: $U =$ 3.30 W/m^{2}K. U-factors calculated for the second greenhouse

window were marked as "preliminary" without explanation. In a companion study (Griffith et al. 1998), measurements were made using a well-insulated greenhouse window constructed from insulating foam (A_s/A_p = 2.35 based on the inside dimensions given or A_s/A_p = 2.12 if A_p is based on the outside dimensions). The surface temperature profile and air flow pattern were measured on the indoor side at the vertical centerline. Neither U nor h_c was measured. In this case, the use of the multi-element model reduced the calculated value of U by 6%, from 1.86 to 1.75 W/m^{2}K.

The results presented by Arasteh et al. (1998) and Griffith et al. (1998) demonstrate, as expected, that U-factors calculated for projecting products will be reduced to some extent if more detail is included when indoor-side radiant heat transfer is modeled. These results also show that the importance of accurately quantifying the indoor side heat transfer coefficient (i.e., both h_c and h_r) decreases as the thermal resistance of the window increases. Arasteh et al. (1998) mention this in their own conclusions. In other words, U can be determined (with little error caused by self-viewing or an inaccurate h_c value) using Equation 3 or 4 as long as the window is well insulated and U itself is small.

It is difficult to draw conclusions regarding the accuracy of the two-dimensional multi-element radiation model because so little information about h_c is known for projecting products. In both of the studies mentioned above, a fixed value of h_c, appropriate for nonprojecting products, was used in lieu of better information. This difficulty is highlighted by the results of Griffith et al. (1998), which showed calculated indoor (warm side) surface temperatures over a large portion of the window falling below measured values. If h_c had also been reduced, and we expect this to be the situation for a projecting product, or if a true three-dimensional model had been incorporated, further reducing h_r, then the discrepancy would have been even larger. Griffith et al. (1998) assert that the "use of a fixed convection film coefficient is causing error in the model" and conclude that "the effect on overall U-factor from incorporating radiation view-factor modeling and local convection film coefficients needs to be validated with hotbox measurements." Finally, it is difficult to determine how much error results from the application of a two-dimensional model to a three-dimensional problem.

OBJECTIVES

In the subsequent sections of this paper, two simple radiant exchange models are developed for application on the indoor side of projecting windows. They are based on classical methods for the analysis of radiant exchange in diffuse, grey enclosures. Both are simple enough to be used as hand calculations, although implementation on a computer adds convenience. Sample calculations are presented to compare one simplified model with the other, to compare the simplified models with the multi-element model described above, and to explore the sensitivity of heat transfer through projecting windows with respect to various design parameters.

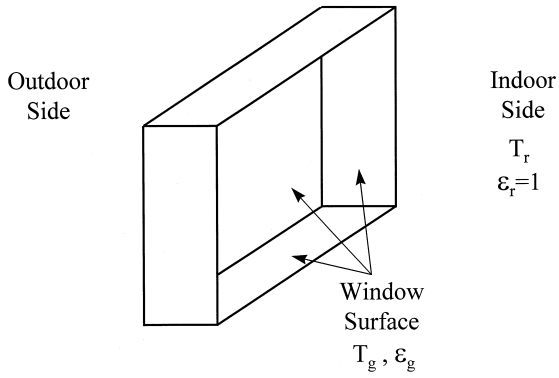

Figure 1a *Perspective of projecting window: single-surface radiation model.*

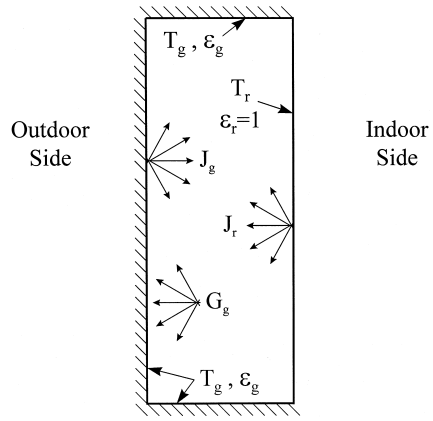

Figure 1b *Details of single-surface radiation model.*

SINGLE-SURFACE MODEL

Consider the arrangement shown in Figure 1. A two-surface enclosure problem is shown where the projecting window is represented by a single surface and the indoor environment represents the second surface. Conventional radiant enclosure analysis entails the idealization that the radiant flux leaving each surface is uniform and diffuse. Therefore, it is assumed that the entire indoor window surface is at a uniform temperature, T_g, has uniform emissivity, ε_g, and is grey (and opaque) in the far infrared wavelength (longwave) band. It is also assumed that surface g, the window, diffusely emits and reflects longwave radiation and it is uniformly irradiated. These assumptions enable the use of radiation shape factors.

The surface of the entire projecting product is assumed to be at temperature T_g even though the floor segment may not be glazed. This is a reasonable assumption because the floor surface will be (a) cooled directly by the outdoor environment if the floor is poorly insulated or (b) cooled by the cold air flowing downward from the glazed surfaces if the floor is well insulated.

An insignificant portion of the radiation directed toward the room from the window surface is reflected back to the window. This is because the room is very large in relation to the window. Therefore, the room can be treated as a black surface ($\varepsilon_r = 1$) with temperature T_r. Furthermore, the room can be represented by a flat surface parallel to the window in the case of a nonprojecting product or by a flat surface located across the open side of a projecting product as if it were the final surface needed to complete an enclosure. This is a particularly useful simplification. More detail regarding the analysis of radiative exchange between a "small object and a large enclosure" (i.e., a window exposed to a large room) can be found in most introductory heat transfer texts. For example, the application of the same simplification, applied specifically to a recessed cavity connected to a large enclosure, is provided in a worked example (Example 13.3) on page 729 of Incropera and DeWitt (1996).

It should be noted that although the room-side surfaces are treated as if they all exist at the same temperature, this does not restrict the applicability of the approach that follows. If it were necessary to account for the presence of unusually hot surfaces (e.g., radiant heaters) or cold surfaces (e.g., other windows), it is possible to subdivide the room into several surfaces, each at a known temperature and known location, and complete the enclosure analysis accordingly. However, in undertaking the thermal analysis of windows, projecting or not, it is very common to assume that the room-side surfaces all exist at the same temperature, and this assumption is used in this analysis.

The radiosity of the window surface (i.e., the radiant flux leaving the surface), J_g, can be expressed in terms of the emitted radiant flux plus the reflected portion of the irradiance (i.e., the radiant flux arriving at the surface), G_g. Note, by Kirchhoff's law, that the reflectance of the surface is $(1 - \varepsilon_g)$, and J_g is

$$J_g = \varepsilon_g \sigma T_g^4 + (1 - \varepsilon_g) G_g \tag{7}$$

where σ = Stefan-Boltzmann constant.

It can be shown that the irradiance at the ith surface, G_i, is given by

$$G_i = \sum_{j=1}^{n} F_{ij} J_j \tag{8}$$

where F_{ij} is the radiation shape factor from surface i to surface j in an enclosure with n surfaces. In this case, G_g is given by

$$G_g = F_{gg} J_g + F_{gr} J_r \tag{9}$$

where F_{gg} is the shape factor from the window to itself, and F_{gr} is the shape factor from the window to the room (i.e., to the window opening). The reciprocity relationship for shape factors gives $A_s F_{gr} = A_p F_{rg}$, and knowing that $F_{rg} = 1$, we have the result $F_{gr} = A_p/A_s$. We also know that $F_{gg} = 1 - F_{gr}$.

The room is treated as a black surface so its radiosity is

$$J_r = \sigma T_r^4. \tag{10}$$

The net flux of radiant energy to the window surface is simply

$$q_g'' = G_g - J_g. \tag{11}$$

Eliminating J_g, J_r, and G_g from Equations 7, 9, 10, and 11 yields[1]

$$q_g'' = \varepsilon_g \sigma (T_r^4 - T_g^4) \left\{ 1 - \varepsilon_g + \frac{\varepsilon_g}{F_{gr}} \right\}^{-1}. \tag{12}$$

The initial portion of this expression ($\varepsilon_g \sigma (T_r^4 - T_g^4)$) can be recognized as the net radiant flux that would be found at the surface of a nonprojecting window. Therefore, the remaining part of the right-hand side can be interpreted as the ratio of radiant heat flux to the surface of the projecting product relative to the radiant heat flux to the surface of the similar nonprojecting product. Calling this factor F_{rad} and replacing F_{gr} by A_p/A_s, we obtain

$$F_{rad} = \frac{1}{1 + \varepsilon_g \left(\frac{A_s}{A_p} - 1 \right)}. \tag{13}$$

This expression illustrates several trends and limiting cases that must be expected to hold. These include the following four items:

- In the trivial case of comparing a nonprojecting product to a nonprojecting product, we have $A_s/A_p = 1$ and expect $F_{rad} = 1$. Equation 13 gives $F_{rad} = 1$.
- If the window surfaces are perfectly reflecting ($\varepsilon_g = 0$), no radiant heat transfer takes place because the window surface can neither emit nor absorb radiation, regardless of window geometry. We expect $F_{rad} = 1$ and Equation 13 yields this result.
- If the window surfaces are black ($\varepsilon_g = 1$), then $F_{rad} = F_{gr} = A_p/A_s$. This indicates, for a fixed value of A_p, that the radiant flux to the window surface diminishes in inverse proportion to A_s. However, the radiant heat transfer from the room to the window is given by the product of q_i'' and A_s and, therefore, does not change as A_s is varied. This makes sense because the window seen from the room will appear to be black regardless of the geometry of the recessed window surfaces.
- With ε_g held constant, F_{rad} always decreases as A_s/A_p increases.

1. This equation can also be obtained using resistance network analysis.

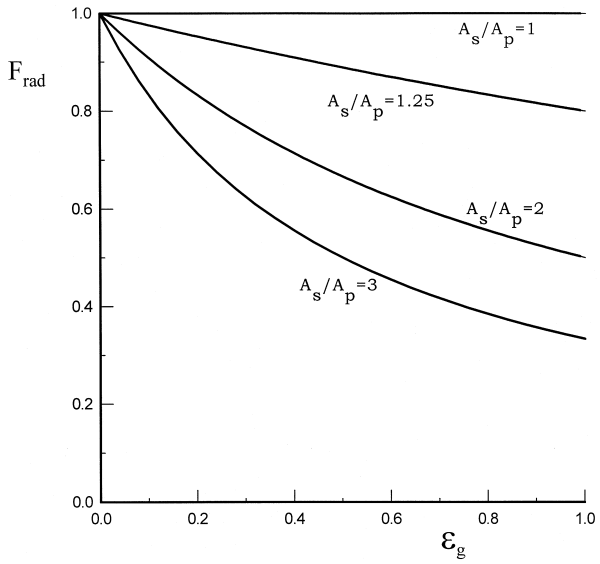

Figure 2 F_{rad} *as a function of* ε_g *and* A_p/A_s, *single-surface model.*

Values of F_{rad} for various combinations of ε_g and F_{gr} are shown in Figure 2. As expected, F_{rad} always falls between zero and unity.

It is of interest to compare this "single-surface model" against the results of the multi-element model used by Arasteh et al. (1998). Consider the first of the two examples presented by Arasteh et al., the poorly insulated greenhouse window. It is assumed that the emissivity of glass can also be used to represent the emissivity of the frame surfaces and we set $\varepsilon_g = 0.84$. The emissivity of most frame surfaces is high, and the area occupied by the frame is small, so this is not expected to introduce an appreciable error. Substituting this emissivity and $1/F_{gr} = A_s/A_p = 2.11$ into Equation 13 gives $F_{rad} = 0.52$. In this case, the indoor side heat transfer coefficient was $h_{in} = 8.3$ W/m^{2}K. The radiant heat flux to the nonprojecting window surface is simply

$$q_r'' = \varepsilon_g \sigma (T_r^4 - T_g^4) \quad (T \text{ in absolute units}). \tag{14}$$

The corresponding radiant heat transfer coefficient is

$$h_r = \varepsilon_g \sigma \frac{T_r^4 - T_g^4}{T_r - T_g} \quad (T \text{ in absolute units}). \tag{15}$$

Using $T_r = 294$ K and $T_g = 286$ K, Equation 15 gives $h_r = 4.65$ W/m^{2}K, and subtracting this value from h_{in} (Equation 6) gives $h_c = 3.65$ W/m^{2}K. Thus, the radiant heat transfer coefficient that should be applied to the projecting product is $h_{r,pp} = F_{rad}h_r = (0.52)(4.65) = 2.40$ W/m^{2}K. A new indoor side heat transfer coefficient for the projecting product, $h_{in,pp}$, is obtained by summing h_c and $h_{r,pp}$, giving $h_{in,pp} = 6.05$ W/m^{2}K.

Assuming that each segment of the projecting product has the same thermal resistance, U_i can be found using Equation 4, yielding $U_i = U/(A_s/A_p) = 10.11/(2.11) = 4.78$ W/m^{2}K. This U-factor corresponds to the indoor heat transfer coefficient $h_{in} = 8.3$ W/m^{2}K. A new estimate of U_i (e.g., $U_{i,pp}$) can be made by developing a thermal resistance circuit to represent the window segment and then replacing h_{in} with $h_{in,pp}$.

$$U_{i,pp} = \left(\frac{1}{U_i} - \frac{1}{h_{in}} + \frac{1}{h_{in,pp}} \right)^{-1} \tag{16}$$

This yields a new U-factor that accounts for the reduced radiant exchange between the projecting window and the indoor environment, $U_{i,pp} = 3.94$ W/m^{2}K. Finally, the new U-factor for the window, U_{new}, can be obtained by using $U_{i,pp}$ in Equation 4, yielding $U_{pp} = U_{i,pp}(A_s/A_p) = 3.94(2.11) = 8.33$ W/m^{2}K. Use of the single-surface model reduces the calculated U-factor by 18% (8.33 vs. 10.11 W/m^{2}K) compared to the 21% reduction (7.95 vs. 10.11 W/m^{2}K) resulting from the use of the multi-element model.

A similar calculation can be applied to the second window sample presented by Arasteh et al. (1998). Results include $h_{r,pp} = F_{rad}h_r = (0.59)(4.65) = 2.73$ W/m^{2}K, $U_{i,pp} = 2.17$ W/m^{2}K, and $U_{pp} = 3.98$ W/m^{2}K. This represents an 8% reduction of calculated U-factor (3.98 vs. 4.32 W/m^{2}K) compared to the 13% reduction (3.75 vs. 4.32 W/m^{2}K) resulting from the use of the multi-element model.

A third calculation was carried out for the foam garden window studied by Griffith et al. (1998). In this case, $\varepsilon_g = 0.9$ was given for the acrylic surface used. Griffith et al. used $h_c = 2.76$ W/m^{2}K and $h_r = 5.05$ W/m^{2}K in their calculations, and the same values were used to generate the results that follow (Equation 15 gives $h_r = 5.0$ W/m^{2}K at $T_r = 294$ K, $T_g = 286$ K, and $\varepsilon_g = 0.9$). Using $A_s/A_p = 2.12$, the single-surface model predicts $F_{rad} = 0.50$, which leads to a 5.4% reduction in calculated U-factor (1.76 vs. 1.86 W/m^{2}K) compared to the 6% reduction (1.75 vs. 1.86 W/m^{2}K) resulting from the use of the multi-element model. If A_s/A_p is taken to be 2.35, the single-surface model gives $F_{rad} = 0.45$ but still predicts $U_{pp} = 1.76$ W/m^{2}K. It is interesting that the reduction in U-factor is not strongly sensitive to the choice of surface-to-projected area ratio. This is true because the window is well insulated and U itself is not strongly influenced by the indoor-side heat transfer coefficient.

TWO-SURFACE MODEL

More detail can be included in a simple calculation by dividing the projecting window into two sections. This arrangement is shown in Figure 3. Surface 1 is the large rectangular section of glazing parallel to the wall and surface 2 consists of the four remaining rectangular segments that connect surface 1 to the wall. The assumptions regarding grey enclosure analysis are the same as those used in the single-surface model. The indoor surface of the window is assumed to be at a uniform temperature, T_g, and again it is noted that $J_r = \sigma T_r^4$. Expressions are written for the radiosity and irradiance at surfaces 1 and 2.

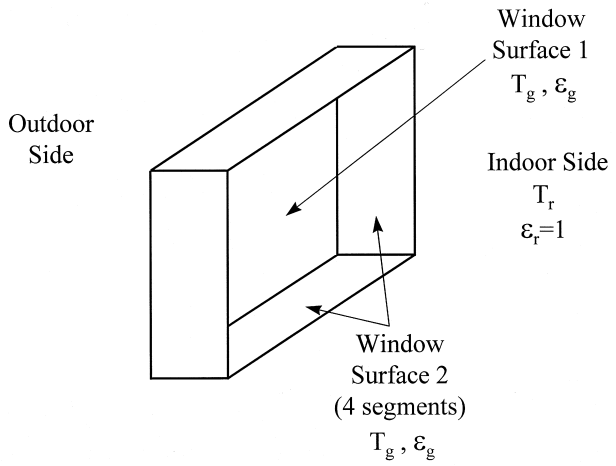

Figure 3a *Perspective of projecting window: two-surface radiation model.*

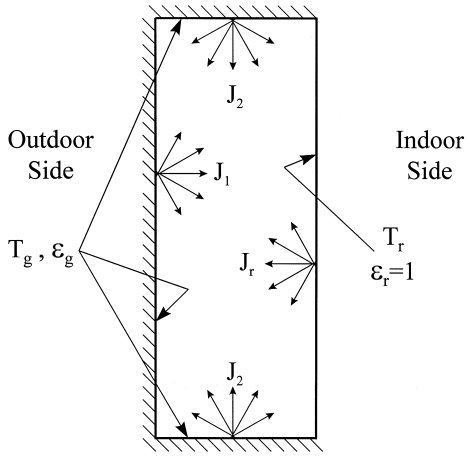

Figure 3b *Details of two-surface radiation model.*

$$J_1 = \varepsilon_g \sigma T_g^4 + (1 - \varepsilon_g) G_1 \tag{17}$$

$$G_1 = F_{11} J_1 + F_{12} J_2 + F_{1r} J_r \tag{18}$$

$$J_2 = \varepsilon_g \sigma T_g^4 + (1 - \varepsilon_g) G_2 \tag{19}$$

$$G_2 = F_{21} J_1 + F_{22} J_2 + F_{2r} J_r \tag{20}$$

Eliminate G_1 and G_2 by substituting Equation 18 into Equation 17 and Equation 20 into Equation 19. J_1 can be eliminated from the two remaining equations while noting that $F_{11} = 0$. This yields the solution for J_2.

$$J_2 = \frac{\varepsilon_g \sigma T_g^4 (1 + (1 - \varepsilon_g) F_{21}) + J_r ((1 - \varepsilon_g) F_{2r} + (1 - \varepsilon_g)^2 F_{21} F_{1r})}{1 - (1 - \varepsilon_g) F_{22} - (1 - \varepsilon_g)^2 F_{21} F_{12}} \tag{21}$$

Once J_2 has been found, back substitution into Equation 18 gives G_1, Equation 17 gives J_1, and Equation 20 gives G_2. Then the radiant flux to each of the two window surfaces can be found.

$$q_1'' = G_1 - J_1 \tag{22}$$

$$q_2'' = G_2 - J_2 \tag{23}$$

and values of F_{rad} for each of the window surfaces can also be found.

$$F_{rad,1} = \frac{q_1''}{\varepsilon_g \sigma (T_r^4 - T_g^4)} \tag{24}$$

$$F_{rad,2} = \frac{q_2''}{\varepsilon_g \sigma (T_r^4 - T_g^4)} \tag{25}$$

The values of $F_{rad,1}$ and $F_{rad,2}$ can now be used to determine new heat transfer coefficients for surfaces 1 and 2.

$$h_{in,pp,1} = h_c + F_{rad,1} h_{r,1} \tag{26}$$

$$h_{in,pp,2} = h_c + F_{rad,2} h_{r,2} \tag{27}$$

These new heat transfer coefficients yield new U-factors, $U_{1,pp}$ and $U_{2,pp}$, according to Equation 16. Finally, the new U-factor for the projecting window is found using Equation 2.

Several shape factors are needed to complete the two-surface model. First, an expression for F_{1r} can be found in many introductory heat transfer texts (e.g., Incropera and deWitt 1996) as the shape factor between opposite sides of a rectangular enclosure. We know that $F_{11} = 0$ so $F_{12} = 1 - F_{1r}$. Reciprocity lets us solve for F_{21} from $A_1 F_{12} = A_2 F_{21}$, and, using symmetry, it can be seen that $F_{2r} = F_{21}$. Finally, $F_{22} = 1 - F_{21} - F_{2r}$.

The two-surface model was applied to the same windows that were examined with the single-surface model. The same values of T_r = 294 K and T_w = 286 K were assumed. The first two windows, the greenhouse windows studied by Arasteh et al. (1998), were constructed with sloped top surfaces (like a small roof section), but this feature was ignored although the depth of the rectangular enclosure used to approximate each of these two windows was adjusted to leave A_s/A_p unchanged. The third window, the foam garden window, was fully rectangular as tested, and no approximation regarding the geometry was needed.

Results generated using the two-surface model are shown in Table 1. The percentages of calculated U-factor reduction resulting from the use of the single-surface model and the multi-element model are also listed in the bottom section of Table 1. Several interesting observations can be made.

- The most striking observation regarding Table 1 is that the two simplified models produce equal amounts of reduction in calculated U-factor, ranging from 5.4% for the foam greenhouse window to 18% for the poorly insulated greenhouse window. See the final two lines of Table 1. It appears that the two-surface model offers no advantage over the single-surface model in this regard.

TABLE 1
Results from Two-Surface Simplified Radiation Model

	Poorly Insulated Window	Moderately Insulated Window	Foam Greenhouse Window
U (W/m^{2}K)	10.11	4.32	1.86
A_s/A_p	2.11	1.83	2.35
h_r (W/m^{2}K)*	4.65	4.65	5.05
h_c (W/m^{2}K)	3.65	3.65	2.76
h_{in} (W/m^{2}K)	8.3	8.3	7.81
F_{1r}	0.601	0.679	0.543
F_{12}	0.399	0.321	0.457
F_{2r}	0.359	0.385	0.338
F_{22}	0.282	0.230	0.324
$F_{rad,1}$	0.627	0.702	0.560
$F_{rad,2}$	0.413	0.445	0.369
$U_{1,new}$ (W/m^{2}K)	4.15	2.23	0.76
$U_{2,new}$ (W/m^{2}K)	3.73	2.09	0.74
U_{new} (W/m^{2}K)	8.31	3.97	1.76
Reduction in Calculated U (%)			
Multi-element model	21	13	6
One-surface model	18	8	5.4
Two-surface model	18	8	5.4

* T_r = 294 K, T_g = 286 K, ε_g = 0.9 for foam window, ε_g = 0.84 otherwise.

- The two-surface model provides extra detail about the nature of the radiant heat transfer. In each case, the one-surface model gives a value of F_{rad} but the two-surface model gives two such values, $F_{rad,1}$ and $F_{rad,2}$, indicating the amounts by which the radiant heat transfer should be reduced at each of surface 1 and surface 2. The values of F_{rad} calculated for the three windows in question all fell between 0.5 and 0.6 (0.52, 0.59, and 0.50). The corresponding values of $F_{rad,1}$ are all higher (0.63, 0.70, and 0.56), and the corresponding values of $F_{rad,2}$ are all lower (0.41, 0.45, and 0.37). This shows that the reduction in radiant heat transfer at surface 1 (the segment facing the room) is less than the reduction at surface 2 (the four perimeter segments). This makes sense because surface 1 is large enough that it "sees" more of the room than the other window surfaces, but each segment of surface 2 "sees" the other segments of surface 2 plus surface 1. This idea can be reinforced by examining the various shape factors and noticing that $F_{1,r}$ is greater than $F_{2,r}$ in each case.
- The simplified calculations provide a slightly smaller reduction in calculated U-factor (from 5.4% to 18%) than the multi-element model (from 6% to 21%). See the last three lines of Table 1. Each calculation method results in better agreement with measurement, but it is not clear which method is more accurate, primarily because the true convective heat transfer coefficient for the projecting product is not known.

APPLICATION OF THE SIMPLIFIED MODELS

In order to apply the simplified models, it is necessary to know, or at least estimate, the indoor surface temperature of the window, T_g. The single-surface model can be used to calculate F_{rad} without knowing T_g (Equation 13), but T_g must be known to determine h_r (Equation 15) and eventually find U_{pp}. The two-surface model requires T_g immediately to calculate $F_{rad,1}$ and $F_{rad,2}$ (Equation 21) and again to determine h_r and U_{pp}.

The sensitivity of the simplified models with respect to the choice of T_g was explored by calculating values of U_{pp} for projecting products corresponding to values of U_i ranging from U_i = 5 W/m^{2}K (a very poorly insulated window segment) down to U_i = 1 W/m^{2}K (a well-insulated window segment) while using three different estimates of T_g. These estimates of T_g were (1) T_g = 290 K, a relatively warm indoor window surface temperature, (2) T_g = 270 K, a cold (below freezing) indoor surface temperature, and (3) T_g was estimated on the basis of the known U-factor by solving the energy balance,

$$h_{in}(T_r - T_g) = U_i(T_r - T_{out}) \tag{28}$$

where the outdoor temperature was set at T_{out} = –17.8°C and the indoor temperature was set at T_{in} = 21.1ºC. The results are shown in Figures 4 and 5 for surface-to-projected area ratios of A_s/A_p = 2 and A_s/A_p = 3, respectively. Note that the single-surface model and the two-surface model produced virtually identical results (U_{pp} typically within 0.1 or 0.2%), so only one set of results is shown in Figures 4 and 5.

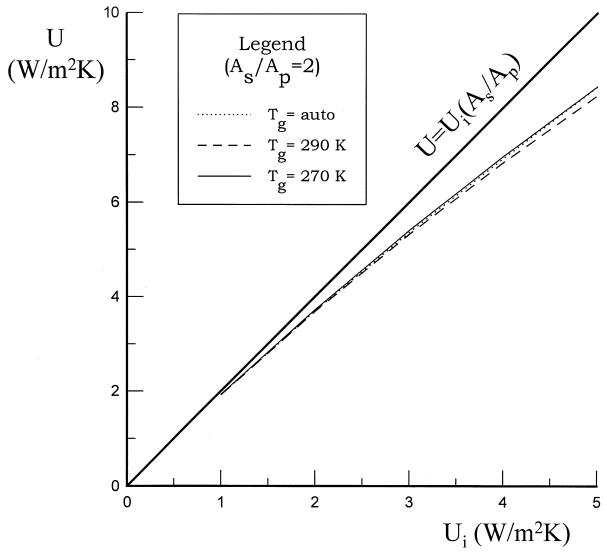

Figure 4 U_{pp} *vs.* U_i, *single-surface model, various values of* T_g, A_s/A_p = *2.*

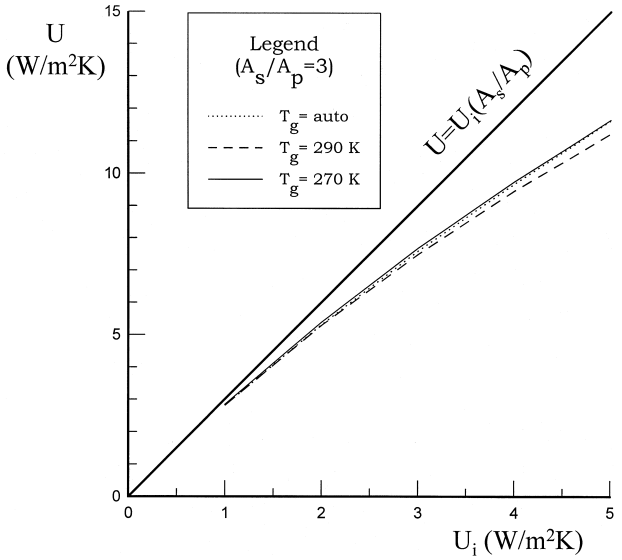

Figure 5 U_{pp} *vs.* U_i, *single-surface model, various values of* T_g, A_s/A_p = *3.*

It is clear, from examining Figures 4 and 5, that the choice of method to estimate T_g is of little importance. In each of these figures, three closely grouped curves show results calculated for each of three values of T_g. Careful examination shows that the uppermost curve corresponds to T_g = 270 K, the lowest curve corresponds to T_g = 290 K, and the results calculated using Equation 28 (T_g = auto) fall in between. The T_g = auto results fall closer to the T_g = 270 K (cold window) when U_i is large (poorly insulated window) as might be expected. When U_i is small, all three results fall in the same place because adjustments in h_{in} have little effect on a well-insulated window. Another expected result is that all three curves approach the straight line that represents Equation 4 as U_i becomes small. This reinforces the idea that it is not necessary to know h_{in} very accurately when a well-insulated window is being considered.

When undertaking glazing system simulation for the purpose of determining U_i, the issue of estimating T_g does not have to be addressed. If the single-surface model is used, F_{rad} can be determined knowing only A_s/A_p and ε_g. Then, the radiative exchange between the surfaces of the projecting product and the room can be reduced by simply substituting a fictitious indoor surface emissivity (e.g., $\varepsilon_{g,fic}$) in place of the true surface emissivity, ε_g (see Equation 15), where

$$\varepsilon_{g,fic} = F_{rad}\varepsilon_g. \tag{29}$$

Thus, the correct T_g is obtained on-the-fly within the calculations undertaken by the customary glazing system analysis, regardless of the particular solution algorithm employed. An improved estimate of h_{in} is provided at the same time, and this, in conjunction with the calculated value of T_g, gives a more accurate calculation of heat loss. This approach is valid as long as the indoor glazing is opaque to longwave radiation (as is glass) and as long as the indoor environment is large so that it can be treated as a black enclosure. These are very common assumptions. This approach can be applied equally well to glazing surfaces or frame surfaces.

If more detail about individual window segments is sought, it is possible to subdivide the window into a number of segments, as demonstrated with the two-surface model, and then to assign a fictitious emissivity to each segment. It would be necessary to estimate T_g in advance in order to calculate the various F_{rad} values, but results in Figures 4 and 5 show that this does not introduce significant error.

CONCLUSIONS

Two simplified radiant exchange models, a single-surface model and a two-surface model, have been developed and demonstrated. These models describe the radiant exchange between the indoor surface of a projecting window and the indoor environment. Either model can be undertaken as a hand calculation or can easily be implemented in existing computer-based simulation techniques.

The two simplified models were shown to produce virtually identical results in predicting U-factors for various projecting products. Therefore, the single-surface model is recommended for heat loss prediction by virtue of its extra simplicity and ease of use. The two-surface model, or similar models incorporating additional segmentation, can be used if additional information about local variation in radiant exchange is of interest.

The results of every model considered confirm that the indoor-side heat transfer coefficient does not need to be accurately known to characterize a well-insulated window.

U-factor reductions predicted by the simplified models agree well with results found in the literature based on a pseudo three-dimensional multi-element computer-based calculation. The use of simplified models gave reductions in calculated U-factor of 18%, 8%, and 5.4% for poorly, moderately, and well insulated greenhouse windows, respectively. The corresponding reductions resulting from the use of the multi-element calculation were 21%, 13%, and 6%. The agreement for the two extreme cases is very good. The discrepancy is larger for the case of the moderately insulated window (8% versus 13%), but it should be noted that the multi-element simulation results published for this particular window were listed as “preliminary,” and this may be where the difference arises. Certainly, any computational approach, simplified or complex, will entail some level of error in relation to reality if some details are omitted (e.g., thermal stratification of the indoor side air). Some details can be neglected if the aim of the calculation is to rate one product versus another.

The U-factor reductions predicted by the simplified models were consistently smaller than the reductions resulting from the use of the multi-element model. It is not clear where these differences originate because various assumptions and approximations are built into each calculation method. It is not

clear which calculation is more accurate because direct comparison with measurement cannot be made until more information is known about the convective heat transfer coefficients for projecting products. Nonetheless, there is a limited amount of evidence to suggest that the U-factor reductions given by the multi-element model are too large (Griffith et al. 1998), lending support to the expectation that the simplified approach is well suited to this application.

It is clear that more research is needed to quantify indoor side convective heat loss to projecting products before indoor-side radiative exchange models can be verified and heat loss through projecting products can be well characterized in general.

ACKNOWLEDGMENTS

This research was supported by the Natural Sciences and Engineering Research Council of Canada and Natural Resources Canada.

REFERENCES

Arasteh, D.K. 1997. Therm 2.0–Internal beta version. Lawrence Berkeley Laboratory, Windows and Daylighting Group.

Arasteh, D.K., E. Finlayson, D. Curcija, J. Baker, and C. Huizenga. 1998. Guidelines for modeling projecting fenestration products. *ASHRAE Transactions* 104 (1B): 854-860.

CEN/ISO. 1999. *prEN ISO 10077-2, Thermal performance of windows, doors and shutters—Calculation of thermal transmittance, part 2: Numerical method for frames.*

CSA. 1993. *CSA A440.2-93, Energy performance evaluation of windows and sliding glass doors.* Rexdale, Ontario, Canada: Canadian Standards Association.

Curcija, D., and W.P. Goss. 1993. Two-dimensional natural convection over the isothermal indoor fenestration surface: Finite-element numerical solution. *ASHRAE Transactions* 99(1): 274-287.

Finlayson, E.U., D.K. Arasteh, C. Huizenga, M.D. Rubin, and M.S. Reilly. 1993. *WINDOW 4.0: Documentation of calculation procedures.* Berkeley, California: Energy and Environment Division, Lawrence Berkeley Laboratory.

Griffith, B.T., D. Curcija, D. Turler, and D. Arasteh. 1998. Improving computer simulations of heat transfer for projecting products using radiation view-factor models. *ASHRAE Transactions* 104(1B): 845-855.

Incropera, F.P., and D.P. DeWitt. 1996. *Fundamentals of heat and mass transfer*, 4th ed. New York: John Wiley & Sons.

NFRC. 1991. NFRC 100-91, Procedure for determining fenestration product thermal properties (currently limited to U-values). Silver Spring, Md.: National Fenestration Rating Council.

Wright, J.L., and H.F. Sullivan. 1995. *VISION4 glazing system thermal analysis—Reference manual.* Waterloo, Ontario, Canada: Advanced Glazing System Laboratory, Department of Mechanical Engineering, University of Waterloo.